

Transfer Function Measurement on the BSC Seismic Isolation Stack

October 07, 1999

Contents

1	Introduction	2
2	Preparation and Properties of Accelerometer	3
3	Experimental setup	4
4	Results	6
4.1	Transmission measurement	6
4.2	Noise measurement on optics table	14
5	Conclusions	16

Chapter 1

Introduction

We present a first set of measurements of the seismic isolation system transfer functions within the Livingston Beam Splitter Chamber 3 (BSC 3). Those measurements are important to probe the reliability of the seismic isolation stack, and test the performance in comparison to the expected grade of isolation. We have tried to take the data under appropriate LIGO conditions - i.e. within the evacuated BSC chamber.

After the installation of the seismic isolation stack in the Livingston, Louisiana, BSC 3 in July 1999, we installed an accelerometer imbedded in a vacuum sealed cavity onto the optics table. The BSC 3 was then closed and the system was pumped to a vacuum of ...??? Four shakers driven by a swept sine input signal were used to exert a force on the construction and the accelerometer response was then detected. The preparation and properties of the accelerometer will be explained in chapter 2. An overview of the experimental setup will follow in chapter 3, and the measurements and results will be discussed in chapter 4.

Though we were not able to get a complete set of data yet, these measurements may give a first idea of the performance of the isolation system. Further measurements have to be taken to confirm and complete the analysis.

Chapter 2

Preparation and Properties of Accelerometer

We used a Wilcoxon 731A Seismic Accelerometer to measure the vertical acceleration on the optical table inside the evacuated BSC 3 chamber. The accelerometer works with a piezoelectric element and is connected to a preamplifier with sensitivity modes of 10, 100 or 1000 V/g.

Preparation:

As the instrument can not be vacuumbaked, it was imbedded into a conical cavity. The parts for the cavity, as well as tools etc. were baked before use and cleaned according to the “LIGO Vacuum Compatibility, Cleaning Methods and Qualification Procedures” (LIGO-E960022-06-E). The accelerometer was cleaned on the outside with isopropanol alcohol before installation on the mounting plate of the cavity. It was mounted flat on the plate as instructed for this type of instrument - with the bottom surface of the accelerometer parallel to the surface of the cavity - on its mounting bolt. The electrical connection was made via two cables as used within the LIGO vacuum system, leading into ports 1 and 13 of the D25 feed-through. Immediately before sealing, the cavity - with accelerometer and cables in place - was carefully filled with neon as a tracer gas. After sealing, a residual gas analysis was performed and showed no neon, so that we are confident not to contaminate the system with substances from inside the cavity. This analysis was after shipping repeated in Livingston prior to installation.

Mounting:

The cavity was mounted onto the optical table with several vacuum-clean clamps and bolts and connected to the outside world via another D25 feed-through in the wall of the BSC tank. Any other instrumentation was assembled outside the chamber.

During all our measurements, the preamplifier was set to 450 Hz low pass, so that above this frequency no data should in any event pass through.

Chapter 3

Experimental setup

In this chapter we will just describe our instrument setup, for a detailed description of the Seismic Isolation Stack see for instance the Preliminary Design Review, LIGO document T960065-03.

Four electromagnetic shakers (Brüel & Kjaer vibration exciters type 4809), with reaction masses of 10 kg each, were attached to the BSC 3 support tubes. The shaker mountings are designed to enable vertical and horizontal installation of shakers and reaction masses, to exert a vertical or horizontal force to the construction, respectively. Each shaker had its own power supply, but all the power sources were connected to the same input signal. This signal was supplied by an HP 780 serving as driving source and as signal analyzer.

The transmission from the support tubes to the optics table within the tank was measured with the accelerometer as described (chapter2). To collect as many excitations as possible that are transmitted from the outside through the seismic isolation system, the accelerometer was mounted off-axis, i.e. it was purposely not installed in the middle of the table, but approximately half way towards the table's outer edge. The accelerometer was connected to the preamplifier as explained in chapter 2. Before going back into the HP 780 another amplifier was used to increase the expected very low signals (model SR 560). Only then was the output from the accelerometer passed back to the HP 780, where the transfer function was stored. An additional oscilloscope served as control panel for signal height and shape.

In a second set of data runs, an accelerometer of exactly the same kind was attached to the mounting of shaker 2 to get the acceleration due to the shaker motion outside the tank. This function was then divided into the transfer function measured on the optics table, to get the real transmission.

All other setups were exactly the same during this second data run.

Transmission measurement from support tube to optics table in the BSC 3:

Three data runs were taken in horizontal shaking mode, i.e. with the shakers exerting a horizontal force onto the construction - from 1-10 Hz, 10-100 Hz and 100 Hz-1kHz. (Note that the measured signal was always vertical acceleration due to the mounting of the accelerometer.) As input signal a frequency swept sine function was used, with the driving voltage differing for the different frequency bands. The driving voltage was always chosen

so that the shakers would be used most efficiently - which means exploiting their whole amplitude in motion ($\pm 4\text{mm}$ reaction mass motion), with the masses just not bumping onto the shakers at lowest frequency (corresponding to strongest motion). From 10 Hz to 1kHz this was the only restriction on the input signal, but for the first band from 1 to 10 Hz - i.e. through the resonances of the seismic isolation stack - special care has been taken not to overexcite the accelerometer. The driving voltage was chosen much lower here (see table 1). In each run, 400 data points were taken and the integration time was set to 5 s or 100 cycles inside the chamber and - for the much stronger signals - 2 s or 40 cycles outside, whichever was bigger.

For settings of the individual instruments and amplification factors see table 1.

Noise measurement on the optics table of BSC 3:

Also included in table 1 are the noise measurements inside the BSC 3 - measured on the optics table with essentially the same setup. The noise output of the accelerometer was measured in two data runs - in a frequency band from 0 - 100 Hz and from 100 - 900 Hz. The HP 780 was now used as pure analyzer in FFT mode. Again, 400 FFT lines were recorded, with averaging 20 times at each frequency to receive the output signal.

Note that for all measurements taken above 450 Hz, there should be no accelerometer output, as the preamplifier of the accelerometer was set to 450 Hz lowpass. Measurements above 450 Hz give just a noise reference e.g. on electronics noise etc.

Transfer functions on optics table and support tube						
run #	position	freq. band	shaker mode	driving volt.	preamp.	amp.
02	inside	100 Hz - 1 kHz	vertical	150 mV	1000 V/g*	100
07	outside	100 Hz - 1 kHz	vertical	25 mV	10 V/g	1
13	inside	10 Hz - 100 Hz	horizontal	150 mV	100 V/g	100
14	inside	100 Hz - 1 kHz	horizontal	150 mV	1000 V/g	100
15	inside	1 Hz - 10 Hz	horizontal	10 mV	1000 V/g	100
17	outside	1 Hz - 10 Hz	horizontal	10 mV	10 V/g	1
19	outside	10 Hz - 100 Hz	horizontal	150 mV	10 V/g	1
20	outside	100 Hz - 1 kHz	horizontal	150 mV	10 V/g	1
Noise measurement on optics table						
03	inside	0 Hz - 100 Hz	no shaking	-	1000 V/g	100
04	inside	100 Hz - 900 Hz	no shaking	-	1000 V/g	100

*constant of gravity taken to be $g = 9.81 \text{ m/s}^2$

Table 1: Settings for relevant data runs. Inside and outside refer to measurements on the optics table within BSC 3 and on the support tube outside the BSC 3, respectively.

Chapter 4

Results

4.1 Transmission measurement

In figure 4.1 we first show the final result of our data runs: the transmission from the support tube to the optical table passing through the seismic isolation stack, driven by the horizontally or vertically exerted force of the shakers. One of the first noticeable features are the high peaks in the lower frequency band at the resonance frequencies of the stack. To understand where those very narrow and steep spikes come from, we plot the transfer functions as measured on the optics table (fig. 4.2) and as measured on the support tube (fig. 4.3), which we divided into each other to receive the transmission from support tube to optics table (so, fig. 4.1 = fig. 4.2/fig. 4.3).

From the number of data points taken (400 per frequency band), due to the logarithmic measuring mode, the frequency resolution ranges as follows in the different bands:

ω [Hz]	$\Delta \omega_{res}$ [Hz]
1 - 10	0.0058 - 0.0575
10 - 100	0.058 - 0.575
100 - 1000	0.58 - 5.75

At the resonance frequencies, we get width for the spikes that are just in the resolution range. For the first peak at 2.8 Hz the local resolution is $\Delta \omega_{res} = 0.016$ Hz, with an $1/\sqrt{2}$ decrease in transmission showing a width of just ~ 0.015 Hz, well below resolution. The same holds for the 6.2 Hz peak, where $\Delta \omega_{res} = 0.036$ Hz compared to a peak width of ~ 0.03 at $1/\sqrt{2}$ of maximum intensity. In contrast to this, the two following peaks at 10.1 and 12.7 Hz are well resolved and show smooth peaks as expected.

We tried to approximate especially the first peak by a simple spring and mass model with internal friction as a damping force. The real geometry of the stack is not taken into account here. This simple model is treated by Saulson (1994) and gives the transmission as:

$$\frac{x}{x_{ground}} = \frac{f_0^2(1+i\Phi)}{f_0^2 - f^2 + i f^2 \Phi}$$

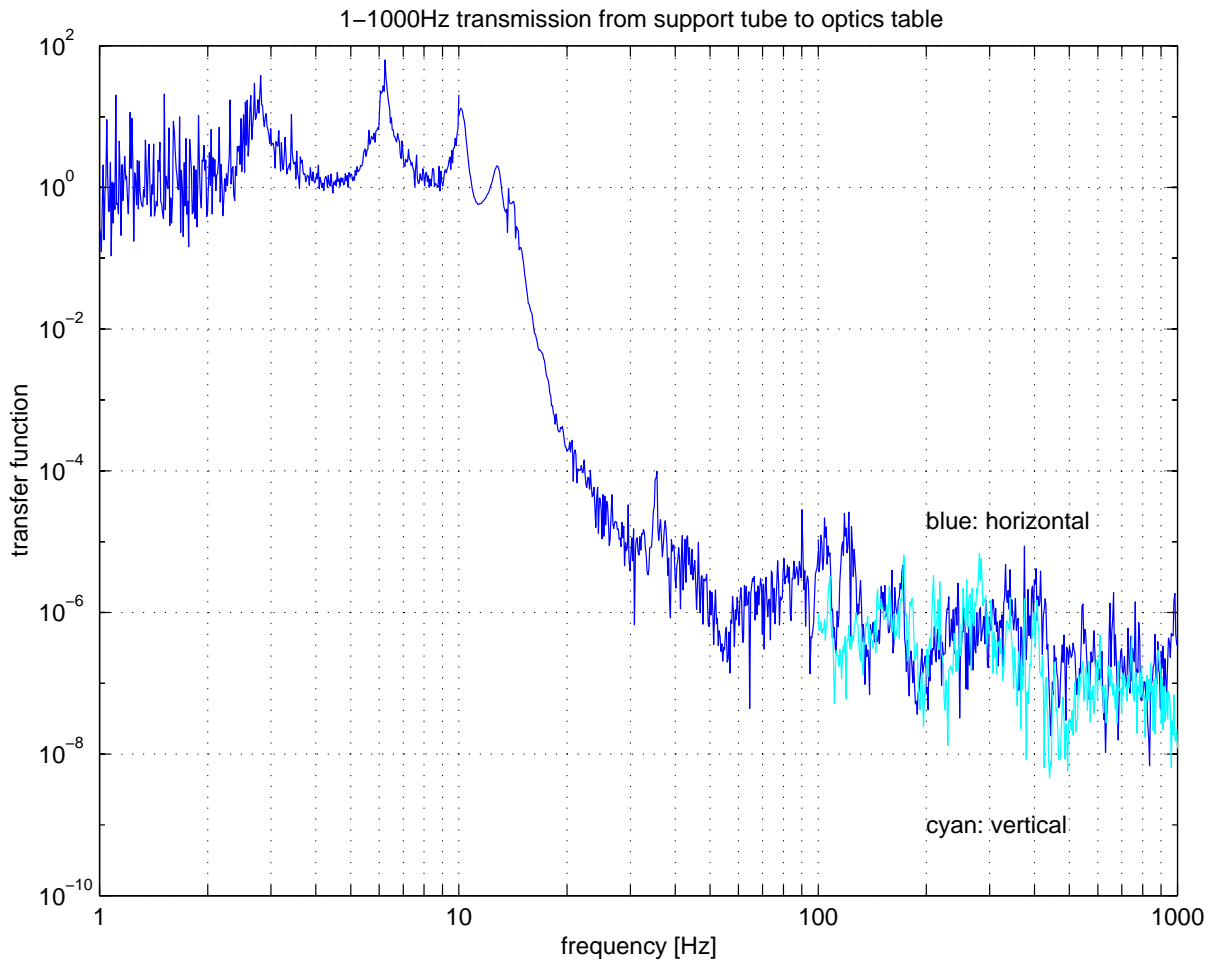


Figure 4.1: Transmission from support tube to optics table of BSC 3. Horizontal and vertical refer to shaker motion (driving force), acceleration was measured vertically off-axis on the optical table (referring to the usual notation, components are T_{zz} and T_{zx} for vertical-vertical (blue) and horizontal-vertical (cyan), respectively).

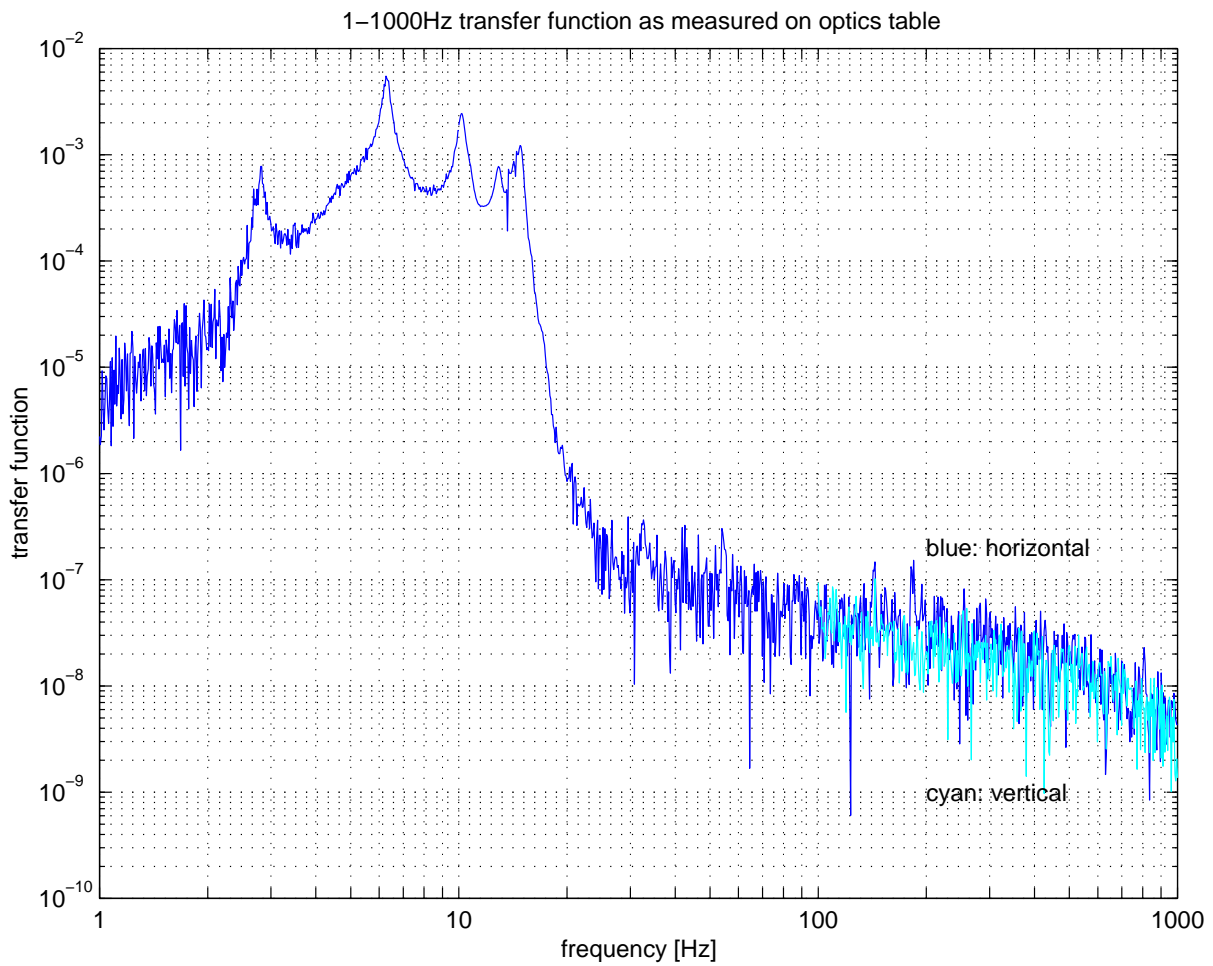


Figure 4.2: Transfer function as measured on the optical table within BSC 3. (else as figure 4.1)

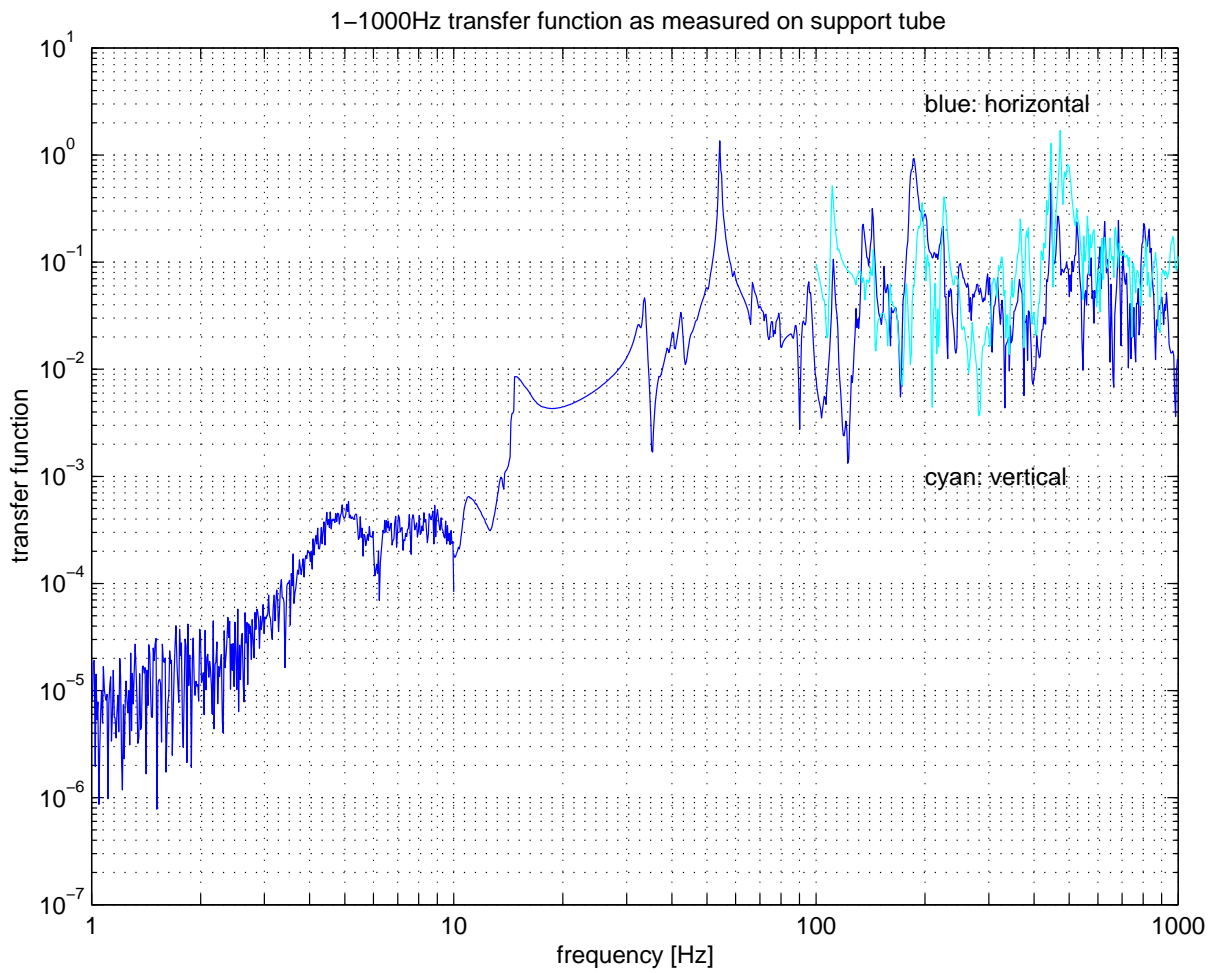


Figure 4.3: Transfer function as measured on the support tube of BSC 3. Acceleration was again measured vertically, with the accelerometer attached to one of the shaker mountings.

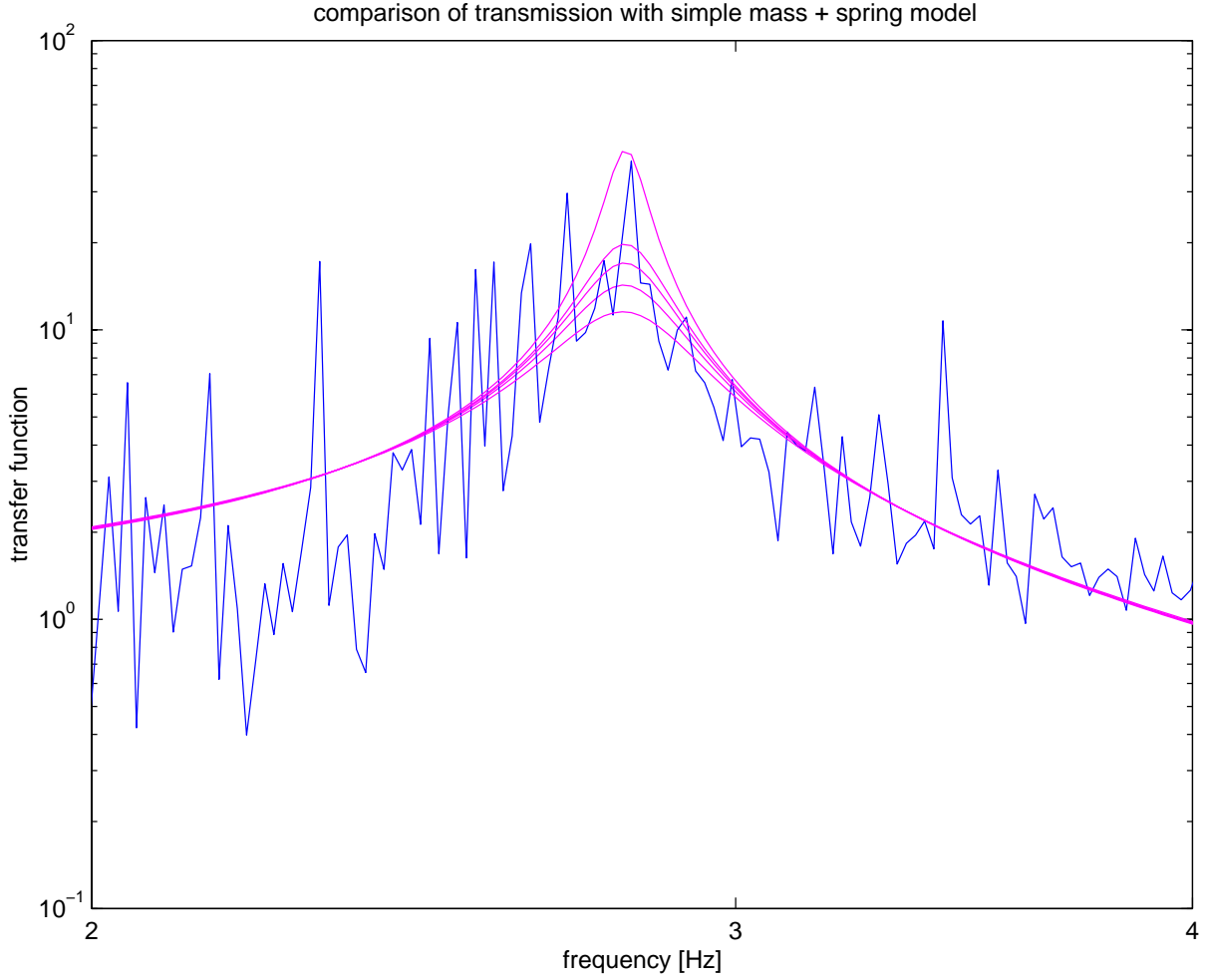


Figure 4.4: Comparison of transmission function with spring and mass model with internal friction as the damping force. Magenta lines are from bottom to top corresponding to Q values of 4,5,6,7 and 15. Note that the wings are the same for all values of Q .

where f is the frequency, f_0 is the resonance frequency and $\Phi \sim 1/Q$.

The theoretical transmission value $|x/x_{ground}|$ is then given by the real part of the above expression:

$$\left| \frac{x}{x_{ground}} \right| = \frac{f_0^2 (1 + \Phi^2)^{1/2}}{((f_0^2 - f^2)^2 + f^4 \Phi^2)^{1/2}}$$

The results of this model are shown in figures 4.5 and 4.6.

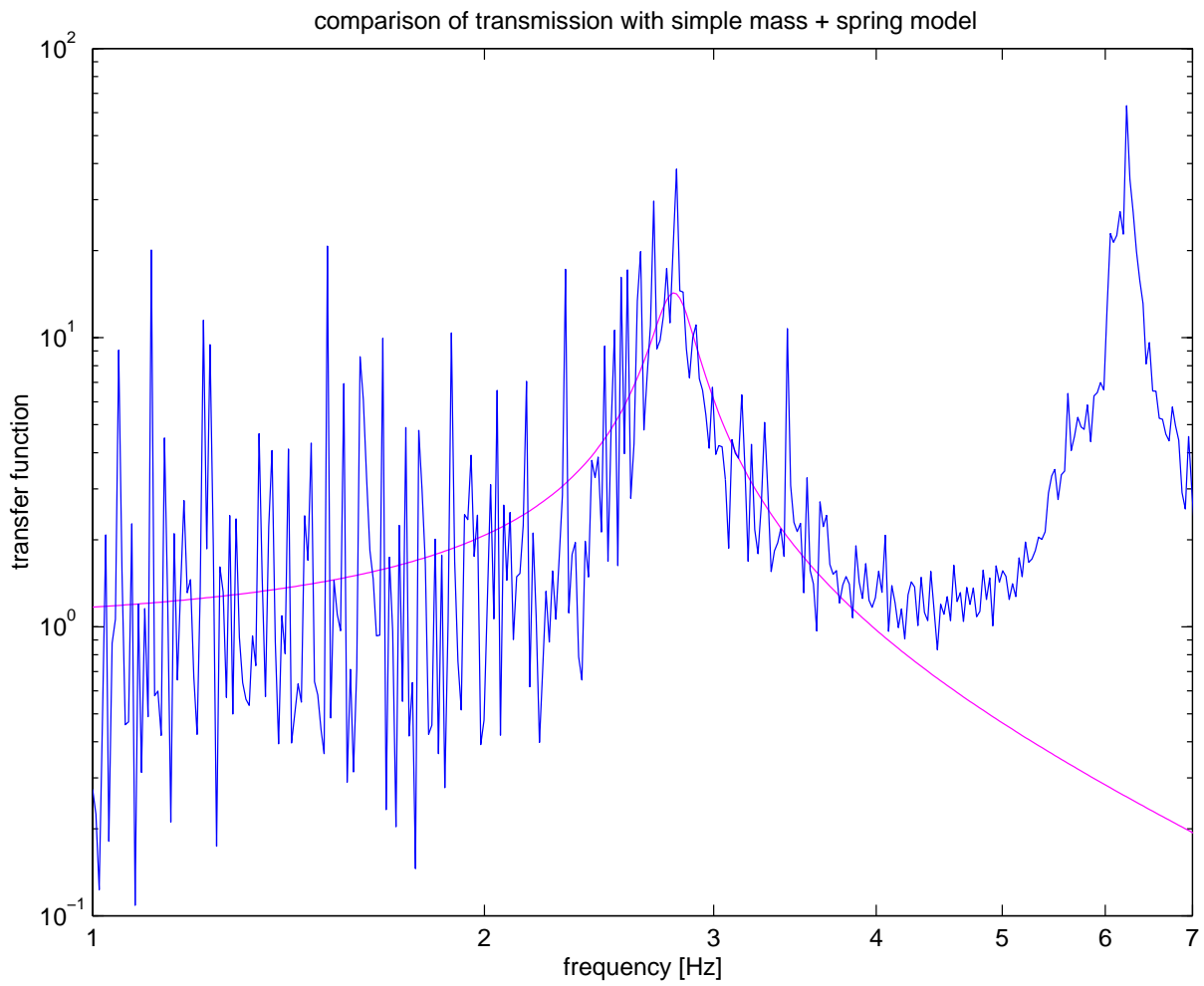


Figure 4.5: The model with $Q = 5$ is shown alone, now with the wings of the resonance peak included.

ω_0 [Hz]	$\Delta \omega$ [Hz]	$Q = \omega_0 / \Delta \omega$	transmission
2.8	-	5 - 7 ¹	14 - 20 ¹
6.2	0.29	21.4 ²	63.4
10.1	0.35	28.8	13.1
12.7	0.57	22.3	2.0

¹rough estimate from model

²rough estimate from below-peak width

Table 2: Q values for the four resonances in the range of 1-10 Hz. For the first two resonances, the values are very rough estimates. The peak transmission is also given. See text for details.

From the first of the two figures we see that from this model the principal shape of the curve is fitted, but it is still hard to determine which value of Q is buried in the data. However, this model gives a good order of magnitude estimate for Qs, we get much more reasonable values than from the spiky peaks considered before. Q values in the range of a few to about 15 may well be close. The second figure shows a broader part of the spectrum, including the wings of the resonance peak. The right wing of the peak towards higher frequencies is very well matched, though on the left side we see the deficiency in the model where the peak rises steeper than is reproduced. Towards lower frequencies the model seems to meet well the average noise level and thus gives an overall good estimate of the first resonance. Distinguishing between one certain value for Q is still difficult, as is obvious in figure 4.5, but there is a hint towards Q values between 5 and 7.

Unfortunately, this method cannot be used for the second resonance at 6.2 Hz, as the whole peak is heavily disturbed by the trough in the transfer function measured on the support tube. The rough estimate given below takes the width of the resonance feature below the spiky top, at the position of the steeply rising flanks, where the width is nearly constant over a wide transmission range. The transmission is here far below the $1/\sqrt{2}$ decrease in intensity - with a value of 20 compared to 62 at the top of the peak. This estimate for Q may be strongly biased and gives just a very rough idea on the possible Q in this resonance. The Q values of the other two resolved resonance features at 10.1 and 12.7 Hertz are determined in the usual way - with the width of the peak measured at $1/\sqrt{2}$ of the maximum transmission. (Note that the spike in the 12.7 Hertz resonance is an artifact due to the end of the measurement run from 1 to 10 Hz.) The final estimates on Q from these data are shown in table 2.

4.2 Noise measurement on optics table

The noise on the optics table in the BSC 3 chamber under vacuum conditions was obtained by recording the accelerometer output without giving any input signal. This situation is comparable to using the seismic noise as driving force. The resonances are again clearly seen. The spectrum shows the decreasing signal from 0.1 to about 20 Hertz, after which the

noise of the setup overtakes the accelerometer output. The FFT mode of the HP 780 was used to make this measurement, averaging 20 times per frequency and recording 400 FFT lines in each of the two data runs, the first from 0.1 to 100 Hz, the second from 100 to 900 Hz. Both data runs are shown in figure 4.7.

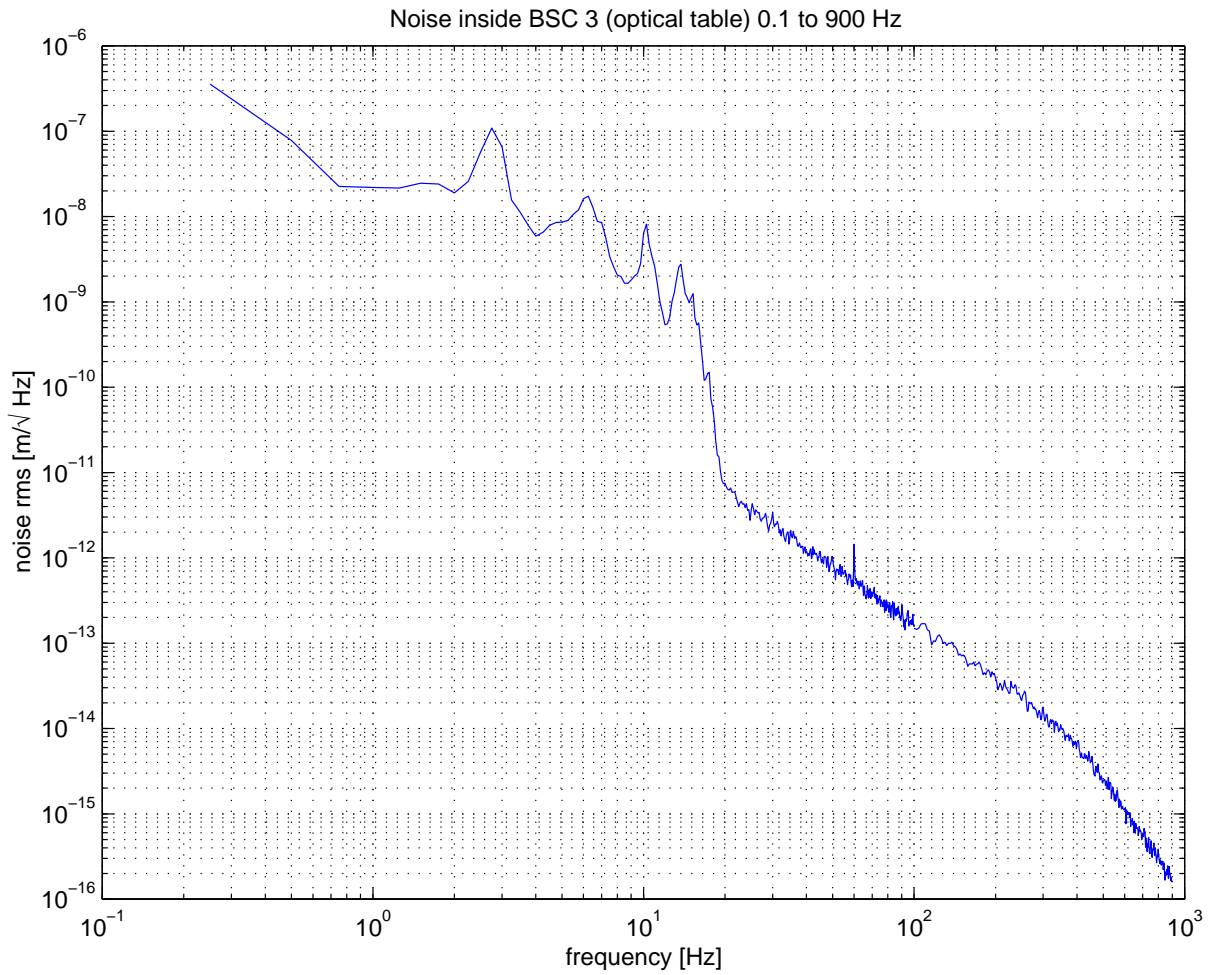


Figure 4.6: Noise measurement on the optics table in BSC 3. Accelerometer output with no applied driving force.

Chapter 5

Conclusions

A series of measurements have been taken in the BSC 3 chamber in Livingston to test the performance of the seismic isolation stack. Though on first sight the resonance peaks occur very steep and spiky, detailed investigation reveals relatively reasonable Q values. The steep falling off after the resonances from about 15 to 20 Hz - towards the point where electrical noise overtakes the accelerometer output - shows the expected behaviour. Unfortunately, we were not yet able to take the full set of data with vertical and horizontal driving, and a measurement of the coherence function has yet to be performed.

References:

Seismic Isolation Stack:

“Preliminary Design Review: Seismic Isolation System”,
LIGO document T960065-03, 1997

for laboratory test on BSC Seismic Isolation Stack:

E. Ponslet, HYTEC

“Transfer Function and Drift Measurements on the BSC First Article Stack”,
HYTEC-TN-LIGO-36, 1998

modelling:

P. Saulson, “Interferometric Gravitational Wave Detectors”,
World Scientific, 1994

Manuals:

Wilcoxon Research 731 A Seismic Accelerometer Operating Guide, 1994

Brüel & Kjaer Vibration Exciter - Type 4809

Accelerometer Preparation:

“LIGO Vacuum Compatibility, Cleaning Methods and Qualification Procedures”
LIGO document E960022-06-E, 1999